

# Accumulation of low-dose BIX01294 promotes metastatic potential of U251 glioblastoma cells

MIN YOUNG KIM<sup>1,2</sup>, SHIN-JI PARK<sup>1</sup>, JAE WOONG SHIM<sup>1</sup>, YU JIN SONG<sup>1</sup>,  
KWANGMO YANG<sup>1,3,4</sup>, SEONG-JOON PARK<sup>1</sup> and KYU HEO<sup>1</sup>

<sup>1</sup>Research Center, Dongnam Institute of Radiological and Medical Science (DIRAMS), Busan 619-953;

<sup>2</sup>Department of Molecular Biology, College of Natural Sciences, Pusan National University, Busan 609-735;

<sup>3</sup>Department of Radiation Oncology, Dongnam Institute of Radiological and Medical Sciences (DIRAMS), Busan 619-953;

<sup>4</sup>Department of Radiation Oncology, Korea Institute of Radiological and Medical Sciences, Seoul 13557, Republic of Korea

Received July 9, 2015; Accepted September 5, 2016

DOI: 10.3892/ol.2017.5626

**Abstract.** BIX01294 (Bix) is known to be a euchromatic histone-lysine N-methyltransferase 2 inhibitor and treatment with Bix suppresses cancer cell survival and proliferation. In the present study, it was observed that sequential treatment with low-dose Bix notably increases glioblastoma cell migration and metastasis. It was demonstrated that U251 cells sequentially treated with low-dose Bix exhibited induced characteristic changes in critical epithelial-mesenchymal transition (EMT) markers, including E-cadherin, N-cadherin,  $\beta$ -catenin and zinc finger protein SNAI2. Notably, sequential treatment with Bix also increased the expression of cancer stem cell-associated markers, including sex determining region Y-box 2, octamer-binding transcription factor 4 and cluster of differentiation 133. Neurosphere formation was significantly enhanced in cells sequentially treated with Bix, compared with control cells (control:  $P=0.011$ ; single treatment of Bix,  $P=0.045$ ). The results of the present study suggest that accumulation of low-dose Bix enhanced the migration and metastatic potential of glioblastoma cells by regulating EMT-associated gene expression, which may be the cause of the altered properties of glioblastoma stem cells.

## Introduction

Glioblastoma is the most common and malignant type of brain tumor in humans, accounting for 50-60% of gliomas and 20% of all intracranial tumors (1). Traditionally, the optimal

treatment strategy for glioblastoma treatment was surgical resection (2). However, due to their highly infiltrative and invasive growth pattern, as well as the existence of multifocal and subclinical lesions, it is difficult to totally eradicate such tumors by surgical resection (2). Concomitant chemotherapy and adjuvant radiotherapy have been used conventionally in the treatment of glioblastoma patients, but the median survival time of these patients remains low (3). One of the major factors contributing to the failures of chemotherapy is the highly infiltrative nature of glioblastoma in normal brain tissue (4). Invasion and metastasis are defining properties of cancer malignancy (5). Due to high invasiveness and metastasis, glioblastoma cells frequently invade the surrounding normal brain tissue, leading to an indistinct boundary between normal brain tissue and glioma tissue (6).

The epithelial-mesenchymal transition (EMT) is a critical cellular process required in normal organogenesis and cellular responses to stress, inflammation and hypoxia. Cancer cells also make use of the mechanisms involved in EMT to undergo invasion and metastasis. The biological processes of EMT include enhanced migratory capacity and invasiveness, elevated resistance to apoptosis, and greatly increased production of extracellular matrix (7-9). EMT is modulated by the repression of E-cadherin, and upregulation of mesenchymal markers, including N-cadherin,  $\beta$ -catenin and zinc finger protein SNAI2 (Slug) (10-12). Furthermore, transition to a mesenchymal gene expression pattern is associated with the simultaneous acquisition of cancer stem cell-like properties (13-15).

BIX01294 (Bix; a diazepin-quinazolinamine derivate) is a euchromatic histone-lysine N-methyltransferase 2 (G9a) inhibitor, and it has been reported that treatment with Bix efficiently blocks cell proliferation and induces autophagy-associated cell death (16,17). However, the effect of persistent low-dose Bix treatment on glioblastoma cell migration and metastasis remains to be elucidated. In the present study, it was shown that sequential treatment with low-dose Bix significantly enhances *in vitro* U251 cell migration, invasion and EMT-associated gene expression. Consistent with the *in vitro* results, following nude mouse experimentation, Bix-treated cells formed larger and more numerous lung tumor metastasis nodules *in vivo*.

---

*Correspondence to:* Dr Kyu Heo or Mr. Seong-Joon Park, Research Center, Dongnam Institute of Radiological and Medical Sciences (DIRAMS), Jwadong-gil 40, Gijang-gun, Busan 619-953, Republic of Korea  
E-mail: khjkh33@gmail.com  
E-mail: kiske223@hanmail.net

**Key words:** BIX01294, metastasis, epithelial-mesenchymal transition, glioblastoma stem cells

Furthermore, neurosphere formation was increased in U251 cells multi-treated with low-dose Bix when compared with untreated and single-treated cells. The results of the present study suggest that characteristic changes were exhibited in the glioma cells exposed to continuous treatment with low-dose Bix.

## Materials and methods

**Cell and culture conditions.** Human glioblastoma cell line U251 was purchased from the American Type Culture Collection (Manassas, VA, USA). Cells were maintained in Dulbecco's Modified Eagle Medium (Welgene, Daegu, South Korea) supplemented with 10% fetal bovine serum (FBS; HyClone; GE Healthcare Life Sciences, Logan, UT, USA) and 5% antibiotic-antimycotic (Gibco; Thermo Fisher Scientific, Inc., Waltham, MA, USA). Cells were cultured at 37°C in a humidified atmosphere of 5% CO<sub>2</sub>.

**Drug treatment.** Stock solutions of 10 mM Bix (Tocris Bioscience, Bristol, UK) were dissolved in dimethyl sulfoxide (DMSO) and diluted in culture medium to 1, 2, 5 and 10  $\mu$ M for cell treatment. For a single treatment of Bix (SBT), the cells were incubated at 37°C overnight, and subsequently treated with 1, 2, 5 and 10  $\mu$ M for 1 day (24 h). For the sequential treatment of Bix (SeBT), the cells were incubated at 37°C overnight, and treated with 1  $\mu$ M Bix. Bix and medium was replaced every 2 days for 2 weeks.

**Cell proliferation assay.** Cell proliferation was assessed using the methyl thiazolyl tetrazolium (MTT) colorimetric assay. U251 cells (2x10<sup>5</sup> cells/well) were seeded in 6-well plates and incubated at 37°C overnight. Following 24 h of incubation, the medium was removed and replaced with the experimental medium. Cells were treated with 1, 2, 5 and 10  $\mu$ M of Bix for SBT or 1  $\mu$ M of Bix for SeBT. Subsequently, cells were washed twice with phosphate-buffered saline (PBS), and 5 mg/ml MTT diluted in PBS was added to each well for a total of 4 h. Following removal of the MTT solution, solubilization solution (DMSO/ethanol, 1:1 ratio) was added to each well to dissolve the formazan crystals. The absorbance at 570 nm was measured using a Paradigm™ Detection Platform (Beckman Coulter, Inc., Brea, CA, USA) and analyzed using Multimode Analysis Software version 3.3.0.9 (Beckman Coulter, Inc.).

**Chromatin isolation by small-scale biochemical fractionation.** Chromatin was isolated from the nuclei of U251 cells. Briefly, 5x10<sup>6</sup> cells were harvested and washed with PBS. The pellet was resuspended in buffer A [10 mM 4-(2-hydroxyethyl)-1-piperazineethanesulfonic acid (pH 7.9), 10 mM KCl, 1.5 mM MgCl<sub>2</sub>, 0.34 M sucrose, 10% glycerol, 1 mM dithiothreitol and protease inhibitor cocktail (Roche Diagnostics, Indianapolis, IN, USA)] with 0.1% Triton X-100. Following an 8-min incubation on ice, nuclei (fraction P1) were collected by centrifugation (1,300 x g for 5 min at 4°C). The P1 nuclei were washed once with buffer A and lysed in buffer B [3 mM ethylenediaminetetraacetic acid, 0.2 mM ethylene glycol-bis ( $\beta$ -aminoethyl ether)-N,N,N',N'-tetraacetic acid, 1 mM dithiothreitol and protease inhibitor cocktail (Roche Diagnostics)] for 30 min. Following lysis, the insoluble

chromatin (fraction P2) and soluble fractions were separated by centrifugation (1,700 x g for 5 min at 4°C). The insoluble P2 fraction was washed once with buffer B and re-suspended in sodium dodecyl sulfate (SDS)-Laemmli buffer and boiled for 10 min. Subsequently, the chromatin samples were quantified by Coomassie Brilliant Blue staining.

**Reverse transcription-quantitative polymerase chain reaction (RT-qPCR) analysis.** RT-qPCR was performed using the SYBR-Green method (18). Total RNA was isolated using the RNeasy Mini kit (Qiagen, Inc., Valencia, CA, USA). The quantity of RNA was measured using a NanoDrop spectrophotometer (Thermo Fisher Scientific, Inc.), and 1  $\mu$ g of RNA was reverse-transcribed using the iScript™ cDNA synthesis kit (Bio-Rad Laboratories, Inc., Hercules, CA, USA). The reaction was performed at 25°C for 5 min, 42°C for 30 min and terminated by heating at 85°C for 5 min. RT-qPCR was performed using a C1000™ thermal cycler (Bio-Rad Laboratories, Inc.) with the Maxima™ SYBR™ Green qPCR master mix (Thermo Fisher Scientific, Inc.). PCR amplification was performed at 94°C for 5 min, followed by 40 cycles of 94°C for 30 sec, 55°C for 30 sec and 72°C for 30 sec.  $\beta$ -actin was used as an internal control (19). To normalize the various RNA samples, the Ct values of  $\beta$ -actin were subtracted from the Ct values of the gene of interest ( $\Delta$ Ct). Then, the  $\Delta\Delta$ Ct values were determined by comparing the  $\Delta$ Ct values of the control and the experimental RNA samples. The following RT-qPCR primers were used: E-cadherin forward, 5'-GTC ACT GAC ACC AAC GAT AAT CCT-3' and reverse, 5'-TTT CAG TGT GGT GAT TAC GAC CTT A-3'; N-cadherin forward, 5'-CAC TGC TCA GGA CCC AGA T-3' and reverse, 5'-TAA GCC GAG TGA TGG TCC-3';  $\beta$ -catenin forward, 5'-GCC ATT TTA AGC CTC TCG GT-3' and reverse, 5'-ATT GTC CAC GCT GGA TTT TC-3'; Slug forward, 5'-AGA TGC ATA TTC GGA CCC AC-3' and reverse, 5'-CCT CAT GTT TGT GCA GGA GA-3'; Kruppel-like factor 4 (KLF4) forward, 5'-GCT GCC GAG GAC CTT CTG-3' and reverse, 5'-AAG TCG CTT CAT GTG GGA GA-3'; cluster of differentiation 133 (CD133) forward, 5'-ACA TGA AAA GAC CTG GGG G-3' and reverse, 5'-GAT CTG GTG TCC CAG CAT G-3'; sex determining region Y-box 2 (SOX2) forward, 5'-TTG CTG CCT CTT TAA GAC TAG GA-3' and reverse, 5'-CTG GGG CTC AAA CTT CTC TC-3'; octamer-binding transcription factor 4 (OCT4) forward, 5'-GTA TTC AGC CAA ACG ACC ATC and reverse, 5'-CTG GTT CGC TTT CTC TTT CG; and  $\beta$ -actin forward, 5'-AGC GAG CAT CCC CCA AAG TT-3' and reverse, 5'-GGG CAC GAA GGC TCA TCA TT-3'.

**Western blot analysis.** Cells were harvested by trypsinization and washed twice with PBS. Subsequently, cell pellets were collected by centrifugation (2,500 x g for 5 min at 4°C) and then lysed by lysis buffer [150 mM NaCl, 20 mM Tris-HCl (pH 7.5), 1% NP40, 5 mM EDTA, 10 mM NAF, 1 mM Na<sub>3</sub>VO<sub>4</sub>, 1 mM DTT and 1X PIC]. The protein concentrations were determined using a Bio-Rad protein assay kit (Bio-Rad Laboratories, Inc.). Cell extracts were boiled in SDS sample buffer (0.5 M Tris-HCl, pH 6.8, 4% SDS, 20% glycerol, 0.1% bromophenol blue and 10%  $\beta$ -mercaptoethanol) and 20  $\mu$ g of protein was loaded onto 4-15% Mini-Protean TGX™ precast gels (Bio-Rad Laboratories, Inc.) and underwent

electrophoresis, followed by transferral to a polyvinylidene difluoride membrane (GE Healthcare Life Sciences, Chalfont, UK). The membranes were blocked with 5% skim milk (BD Biosciences, San Jose, CA, USA) at room temperature for 30 min, and incubated overnight at 4°C with the primary antibodies. On the following day, the membranes were washed with TBS-T (20 mM Tris, 137 mM NaCl, pH 7.6, 0.2% Tween 20) for 10 min, 3 times each, and incubated with the secondary antibody at 37°C for 1 h: goat-anti-rabbit horseradish-peroxidase conjugated antibody (dilution, 1:5,000; catalog no., ab6721, Invitrogen; Thermo Fisher Scientific, Inc.) or rabbit-anti-mouse horseradish-peroxidase conjugated antibody (dilution 1:5,000; catalog no., ab97046, Invitrogen; Thermo Fisher Scientific, Inc.). The immunoreactive proteins were detected using enhanced chemiluminescence (Thermo Fisher Scientific, Inc.). Immunoblots were quantified using the Fusion FX5 system (Vilber Lourmat, Marne, France). The following primary antibodies (dilution, 1:1,000) were used for immunoblot analysis: anti-poly (ADP-ribose) polymerase (PARP) (catalog no. sc-7150; Santa Cruz Biotechnology, Inc., Dallas, TX, USA), anti-caspase-3 (catalog no. 9662; Cell Signaling Technology, Inc., Danvers, MA, USA), anti-microtubule-associated protein light chain 3 (LC3) B (catalog no. #3868; Cell Signaling Technology, Inc.), anti-histone H3 (catalog no. ab1791; Abcam, Cambridge, UK), anti-dimethyl-histone H3-Lys9 (catalog no. 07-212; Merck Millipore, Darmstadt, Germany), anti-E-cadherin (catalog no. sc-7870; Santa Cruz Biotechnology, Inc.), anti-N-cadherin (catalog no. 610921; BD Biosciences), anti- $\beta$ -catenin (catalog no. 610153; BD Biosciences), anti-Slug (catalog no. sc-166476; Santa Cruz Biotechnology, Inc.), anti-KLF4 (catalog no. ab72543; Abcam), anti-CD133 (catalog no. ab19898; Abcam), anti-SOX2 (catalog no. sc-20088; Santa Cruz Biotechnology, Inc.), anti-OCT4 (catalog no. 611203; BD Biosciences) and anti- $\beta$ -actin (dilution, 1:5,000; catalog no. A5441; Sigma-Aldrich; Merck Millipore).

**Migration and invasion assays.** Cell migration and invasion assays were performed using Transwell® chambers (8- $\mu$ m pore size; Corning Life Sciences, Lowell, MA, USA). A total of  $2 \times 10^4$  cells were resuspended in 0.2 ml of serum-free growth medium for both the cell migration and invasion assays. For the migration assay, the cells were added to the interior of the inserts. Growth medium (0.8 ml) supplemented with 10% (v/v) FBS was added to the lower chamber. Following 24 h incubation at 37°C, the cells attached to the upper surface of the filter were removed using a cotton swab, and migratory cells on the lower surface of the filter were fixed and stained for 15 min with 0.25% crystal violet (Merck Millipore), 10% formaldehyde, and 80% methanol. Subsequently, the inserts were washed 5 times with double-distilled H<sub>2</sub>O and photographed (magnification, x200). Migrated cells were determined by counting cells in 5 microscopic fields (randomly selected) per well and the extent of migration was expressed as the mean number of cells per microscopic field (20). Cells were imaged using phase contrast microscopy (Nikon Eclipse 80i; Nikon Corporation). For the invasion assay, cells were added to the interior of the inserts pre-coated with 10 mg/ml growth factor-reduced Matrigel™ (BD Biosciences). Growth medium (0.8 ml) supplemented with 10% (v/v) FBS was added to the

lower chamber. Following 24 h incubation at 37°C, the inserts were processed as described above for the migration assay.

**Sphere formation assay.** U251 cells were suspended at a density of 5,000 cells/well in complete NeuroCult™ NS-A Basal media (Stemcell Technologies, Inc., Vancouver, BC, Canada) and plated in triplicate wells on a 24-well ultra-low attachment culture plate (Corning Life Sciences). Cells were incubated at 37°C for 7-10 days. The number of spheres was imaged using inverted microscopy (Nikon Eclipse TS 100, Nikon Corporation) and sphere diameters were determined using Image-Pro Plus version 7.0 software (Media Cybernetics, Rockville, MD, USA).

**In vivo experiments.** Female 6-week-old nude BALB/c mice were obtained from Japan SLC, Inc. (Hamamatsu, Japan), and were raised under following conditions (temperature, 22±2°C; humidity, 50±10%; access to food, *ad libitum*; light/dark cycle, 12/12 h). All animal protocols used in this study were approved by the Institutional Animal Care and Use Committee at Dongnam Institute of Radiological & Medical Sciences (DIRAMS; Busan, Republic of Korea). Female BALB/c nude mice (average weight, 22 g; n=27) were randomly divided into three groups (control, SBT and SeBT). Control- or single/sequential-Bix treated U251 cells ( $2 \times 10^6$  cells) were inoculated intravenously into BALB/c nude mice. After 4 weeks, the mice were sacrificed using anesthesia and exsanguination, and lungs were corrected by dissection.

**Statistical analysis.** All statistical analyses were performed using Microsoft Excel 2007 (Microsoft Corporation, Redmond, WA, USA). Student's *t*-test was used for statistical comparisons. *P*<0.05 was considered to indicate a statistically significant difference.

## Results

**Sequential treatment with Bix does not affect cell viability in human U251 glioblastoma cells.** Bix has been reported to have antiproliferative effects in various types of cancer cell (16,17). Therefore it was initially examined whether Bix treatment inhibited the proliferation of U251 glioblastoma cells. U251 cells were prepared according to the experimental scheme shown in Fig. 1A. Subsequently, viability of cells was assessed by the MTT assay. When cells were treated with 1, 2, 5 and 10  $\mu$ M Bix, the viability of U251 cells decreased in a dose-dependent manner (*P*=0.143, *P*=0.001, *P*=0.002 and *P*=0.001, respectively) (Fig. 1B). To investigate whether accumulation of non-lethal doses of Bix led to changes in cell survival rates, U251 cells were exposed to sequential low-dose (1  $\mu$ M) Bix treatment. Notably, U251 cell viability was unaffected by multiple low-dose treatments of Bix (Fig. 1B). As Bix has been observed to attenuate G9a activity (17), the effect of Bix on H3K9 dimethylation levels was initially examined. The results revealed that the single treatment of Bix decreased the levels of H3K9 demethylation, whereas sequential treatment of Bix had no such effect (Fig. 1C). Expression levels of apoptosis- and autophagy-associated proteins were also measured by western blot analysis following treatment with various concentrations of Bix. The results of the present study

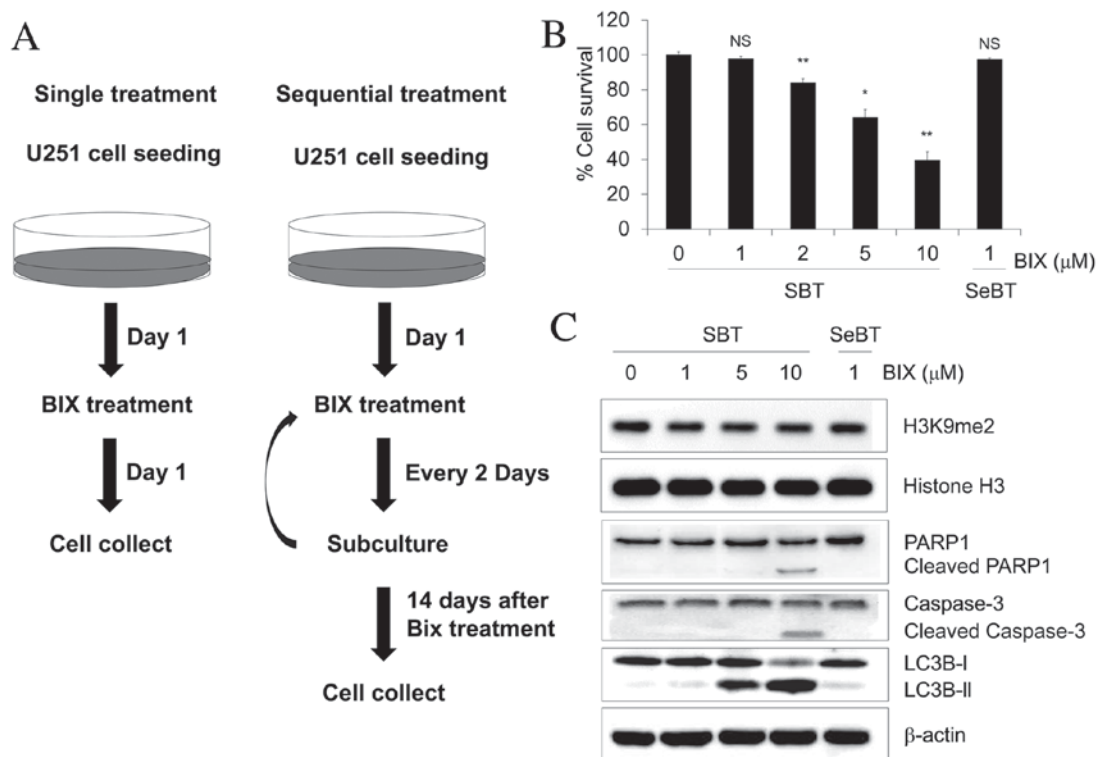


Figure 1. Cell survival effect of Bix treatment following the indicated dosing schedule in human U251 glioblastoma cells. (A) Experimental scheme for Bix treatment. (B) The cells were treated with 1, 2, 5 or 10  $\mu$ M Bix and the methyl thiazolyl tetrazolium assay was performed. (C) Levels of dimethylated H3K9 and apoptosis/autophagy-associated genes investigated by western blot analysis. Relative optical densities of dimethylated H3K9 level were normalized to total histone H3 (1,  $0.88 \pm 0.01$ ,  $0.80 \pm 0.05$ ,  $0.91 \pm 0.03$ ,  $0.92 \pm 0.1$ , respectively, mean  $\pm$  standard error of the mean).  $\beta$ -actin was used as the loading control. Western blotting was performed at the indicated dosages (0, 1, 5 and 10  $\mu$ M). Bix, BIX01294; SBT, single treatment of Bix; SeBT, sequential treatment of Bix; PARP, poly (ADP-ribose) polymerase. P-values were calculated using the Student's *t*-test. \* $P < 0.01$  vs. the control; \*\* $P < 0.001$  vs. the control; N.S. no significance.

demonstrated that a single treatment with 10  $\mu$ M Bix in U251 cells induced PARP1 and caspase-3 cleavage, whereas the cleavage of PARP1 and caspase-3 was not stimulated with sequential treatment with 1  $\mu$ M Bix (Fig. 1C). LC3B is widely used as a biomarker of autophagy, during which, LC3B-I is converted to LC3B-II through lipidation by a ubiquitin-like system that allows LC3B to become associated with autophagic vesicles (21). Similar to PARP1, the conversion of LC3B-I to LC3B-II was only induced with high doses of Bix (5 and 10  $\mu$ M), and not with the sequential treatment of low-dose Bix (Fig. 1C). These results indicate that accumulation of low doses of Bix does not influence U251 cell proliferation and apoptosis.

**Sequential treatment with low-dose Bix enhances migration and invasion of U251 cells.** Subsequently, the effect of sequential treatment with low-dose Bix (1  $\mu$ M) on the migration and invasion capability of U251 glioblastoma cells was investigated. As presented in Fig. 2A and B, SBT cells exhibited an approximately 3-fold increase in the number of migratory cells ( $P = 0.011$ ), compared with untreated control cells, whereas SeBT cells showed an approximately 12-fold increase ( $P = 0.044$ ). Similarly, SeBT cells exhibited a 2.5-fold increase in the number of invasive U251 cells, compared with control cells ( $P = 0.001$ ) (Fig. 2A and B). As the ability to invade and migrate is correlated with EMT capacity (22), the expression levels of EMT-associated factors such as E-cadherin, N-cadherin, Slug and  $\beta$ -catenin were evaluated

by RT-qPCR (Fig. 2C) and western blotting (Fig. 2D) in SBT and SeBT cells. The expression of E-cadherin was demonstrably decreased following SeBT, compared with the control ( $P = 0.008$ ) and SBT ( $P = 0.002$ ), whereas the expression of N-cadherin and  $\beta$ -catenin was significantly increased following SeBT compared with the control (N-cadherin,  $P < 0.001$ ;  $\beta$ -catenin,  $P < 0.001$ ) and SBT (N-cadherin,  $P = 0.004$ ;  $\beta$ -catenin,  $P = 0.007$ ). In the case of Slug, the expression was marginally increased by SeBT, compared with the control (Fig. 2C and D). The results of the present study suggest that accumulation of low-dose Bix induces invasion and migration, as well as EMT, in U251 cells.

**Sequential treatment with Bix enhances U251 cell pulmonary metastasis in vivo.** To investigate the impact of sequential treatment with Bix on U251 cell metastasis, a pulmonary metastasis experiment was performed. A total of  $2 \times 10^6$  control, SBT or SeBT U251 cells were intravenously injected into nude BALB/c mice. After 4 weeks, the mice were sacrificed as described in the materials and methods section, and lung tissues were visualized (Fig. 3A, left panel). The results showed that the mice injected with SeBT cells had larger sized nodules in lung tissue, compared with mice injected with control ( $P = 0.013$ ) or SBT ( $P = 0.022$ ) cells. Furthermore, the largest number of metastatic lung nodules was observed in mice injected with SeBT cells (Fig. 3A, right panel). Induced nodule formation by sequential treatment with Bix was also observed in tissue sections (Fig. 3B). The

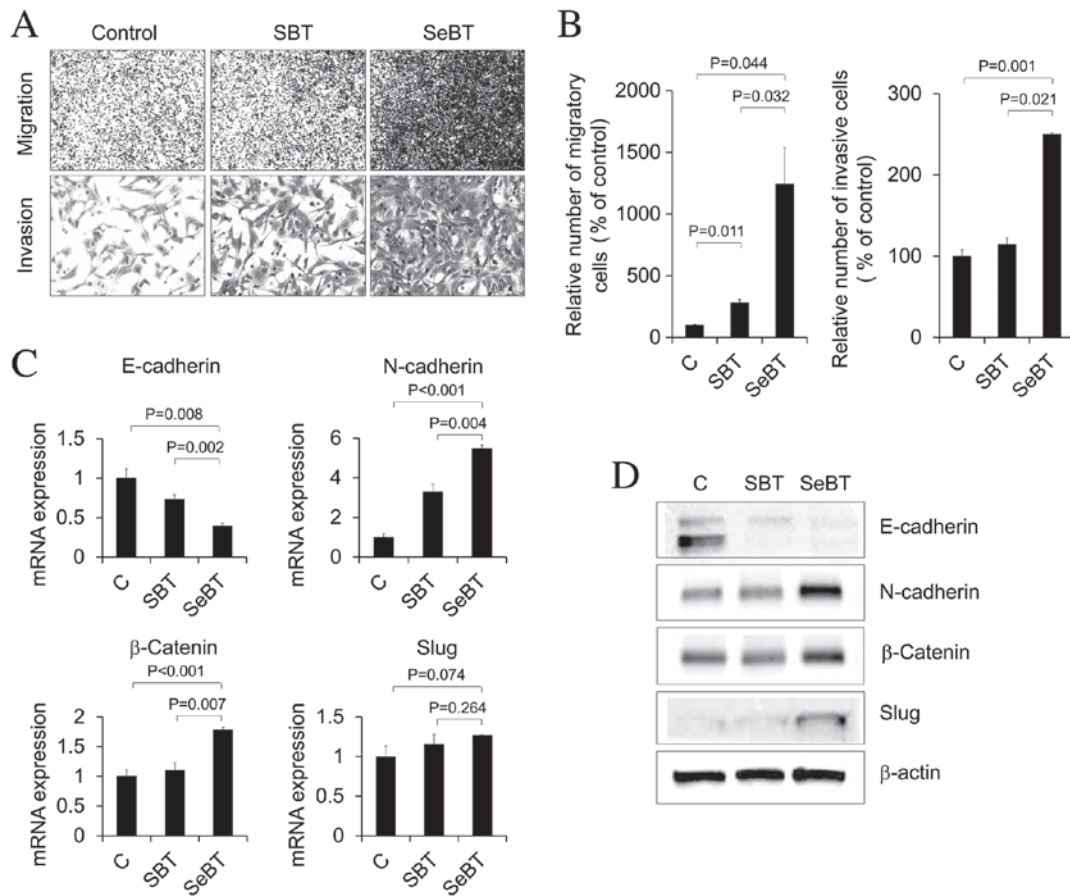


Figure 2. Enhanced cellular migration and invasion following sequential treatment with Bix in U251 cells. (A) Images of migratory (upper panel) and invasive (bottom panel) cells under phase contrast microscopy (magnification, x200) are shown. (B) The number of migratory and invasive cells was counted and presented. Values are presented as the mean  $\pm$  standard deviation. Representative data from three independent trials. (C) E-cadherin, N-cadherin,  $\beta$ -catenin and Slug mRNA expression patterns under SBT or SeBT were assessed by reverse transcription-quantitative polymerase chain reaction analysis. Results represent mRNA levels normalized to the levels of  $\beta$ -actin mRNA. Relative E-cadherin, N-cadherin,  $\beta$ -catenin and Slug mRNA levels are presented as the mean  $\pm$  standard deviation of three independent experiments. (D) Western blot analysis demonstrated the change in total protein expression of E-cadherin, N-cadherin,  $\beta$ -catenin and Slug. The expression level of  $\beta$ -actin was used as loading control. Bix, BIX01294; SBT, single treatment of Bix; SeBT, sequential treatment of Bix; Slug, zinc finger protein SNAI2; C, control.

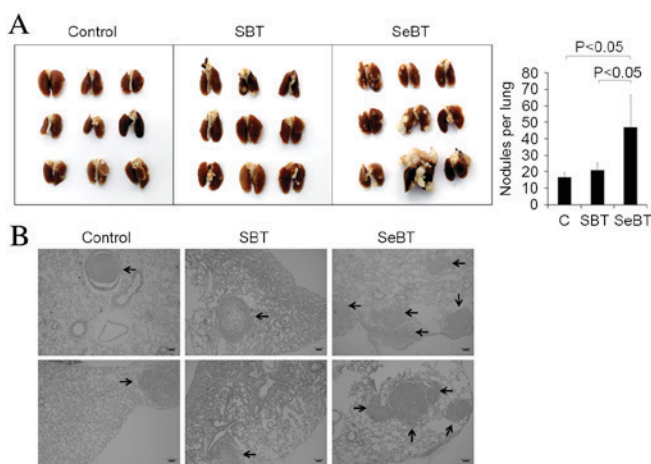


Figure 3. Sequential treatment with Bix increases tumor metastasis in nude BALB/c mice. (A) U251 cells ( $2 \times 10^6$ ) were injected subcutaneously into nude mice (n=9). A total of 4 weeks following injection, lung tissue of sacrificed mice was visualized. Representative images comparing lung tissues between untreated cells and SBT/SeBT cells (left panel). The graph indicates the number of metastatic lung nodules in single or sequential Bix injected mice (right panel). (B) Representative images (hematoxylin and eosin stain; magnification, x200) show histological changes in the lung tissue and block arrows represent the lung nodules. Bix, BIX01294; SBT, single treatment of Bix; SeBT, sequential treatment of Bix; C, control.

results of the present study support the idea that accumulation of low-dose Bix enhances the ability of U251 cells to migrate and metastasize.

*Sequential treatment with Bix increases the expression of cancer stem cell markers and neurosphere formation.* CD133 is a critical marker of self-renewal in glioblastoma cells and its expression has been implicated in tumorigenic potential, as well as metastatic ability (23). KLF4, SOX2 and OCT4 also have essential roles in stem cell biology (23). To investigate whether the SeBT-induced metastatic potential of U251 cells has any correlation with stem cell-like properties, the expression of these markers was identified using RT-qPCR (Fig. 4A). The expression of CD133, SOX2 and OCT4 was significantly upregulated in SeBT cells, compared with the control (P=0.001, P=0.002 and P=0.001, respectively) and SBT (P=0.021, P=0.096 and P=0.015, respectively) cells. By contrast, the expression of transcription factor KLF4 was decreased in SeBT cells, when compared with control (P=0.003) and SBT (P=0.009) cells (Fig. 4A). Similar patterns were observed in western blot analysis (Fig. 4B). These data demonstrate that SeBT of cancer cells may induce cancer stem cell expansion. As glioma stem cells have been reported to

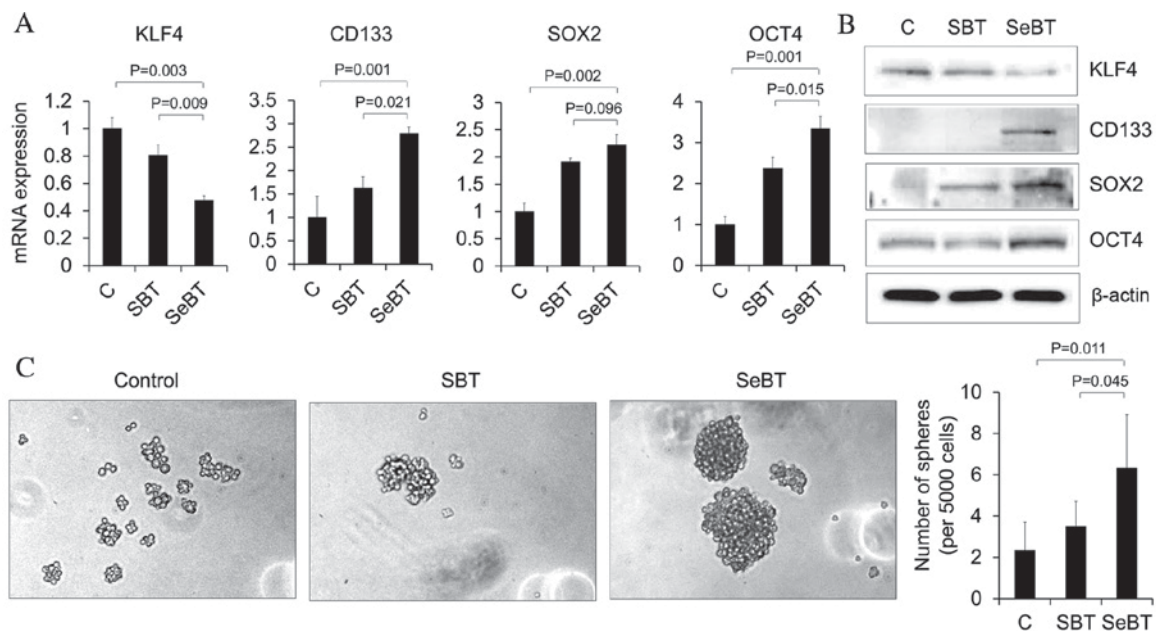


Figure 4. Sequential treatment with Bix increases the expression of cancer stem cell markers and neurosphere formation in U251 cells. (A) KLF4, CD133, SOX2 and OCT4 mRNA expression patterns under single or sequential treatment with Bix were assessed by reverse transcription-quantitative polymerase chain reaction. Results represent mRNA levels normalized to the levels of  $\beta$ -actin mRNA. Relative KLF4, CD133, SOX2 and OCT4 mRNA levels are presented as the mean  $\pm$  standard deviation of three independent experiments. (B) Western blot analysis demonstrated the change in total protein expression of KLF4, CD133, SOX2 and OCT4. The expression level of  $\beta$ -actin was used as loading control. (C) Representative images of neurosphere formation following single or sequential treatment of Bix. Bix, BIX01294; KLF4, Kruppel-like factor 4; CD133, cluster of differentiation 133; SOX2, sex determining region Y-box 2; OCT4, octamer-binding transcription factor 4; SBT, single treatment of Bix; SeBT, sequential treatment of Bix; C, control.

form neurospheres at an increased efficiency compared with differentiated cells, the present study sought to determine the effect of SeBT cells on sphere formation, as this may be an indicator of a cancer stem cell-like phenotype. Control, SBT or SeBT cells were seeded on 24-well low adhesion plates at a density of 5,000 cells per well, and after 1 week, spheres were visualized (Fig. 4C). It was demonstrated that SeBT cells formed a greater number of spheres, compared with control ( $P=0.011$ ) and SBT ( $P=0.045$ ) cells. In addition, SeBT cells formed larger spheres, compared with control and SBT cells. The results of the present study suggest that prolonged exposure to low-dose Bix induces metastatic potential and self-renewal in U251 cells.

## Discussion

Glioblastoma is characterized by rapid cell proliferation, as well as high invasion and migration properties (24). The median survival time of glioblastoma is 6-14 months; in addition to this, a 2-year survival rate is observed in only 10% of patients and 5-year survival is observed in <5% (25). Previously, advanced chemotherapy and adjuvant radiotherapy have been used to treat glioblastoma patients, but the response is generally unfavorable and the toxic chemotherapy and radiotherapy frequently produce serious adverse side effects (26). The primary cause of treatment failure is invasion and metastasis of glioblastoma into normal brain tissues (4).

In the present study, it was demonstrated that accumulation of low-dose Bix induces the migratory and invasive phenotype in U251 glioblastoma cells. The results of the present study revealed that Bix inhibited proliferation and induced apoptosis in U251 cells in a dose-dependent manner.

However, multiple treatments of low-dose Bix did not influence cell survival or apoptosis. Although accumulation of damage by sequential treatment with non-lethal doses of Bix was not able to change the cell proliferation rate, SeBT cells exhibited an increased migratory and invasive phenotype compared with control or SBT cells. EMT is a critical event in the development of invasive and metastatic potential in cancer progression (6). EMT is known to be initiated through the regulation of the Wnt/ $\beta$ -catenin, transforming growth factor- $\beta$ , Smad, Notch and Hedgehog signaling pathways (22,27,28). This complex signaling network begins with the cleavage of E-cadherin, which causes adherent junction breakdown and an indirect increase in the expression of transcription factors, including Slug and  $\beta$ -catenin. The repression of the epithelial gene E-cadherin indirectly leads to an increase in the expression of N-cadherin and other mesenchymal genes (29). It was also demonstrated that enhanced migratory and invasive ability, which is exhibited by SeBT cells, was accompanied by downregulation of E-cadherin, and upregulation of N-cadherin and  $\beta$ -catenin. This indicated that the EMT process is involved in the induced migration and invasion of SeBT cells. Notably, the mRNA expression level of Slug was not markedly altered between SBT and SeBT cells. However, the protein level of Slug was upregulated in SeBT cells. Furthermore, these gene expression changes were not directly induced by the Bix-mediated inhibition of G9a, as H3K9 dimethylation levels were not correspondingly altered. The results of the present study suggest that there may be another regulatory mechanism of Bix, leading to EMT stimulation. In order to confirm this phenomenon *in vivo*, treated U251 cells were injected into nude mice via the tail vein. The results revealed

that SeBT cell-injected mice had more and larger nodules compared with control and SBT cell-injected mice. Expansion of cancer stem cells also enhances the invasive and metastatic potential of cancer cells (28). Cancer stem cells are tumor-initiating cells found in the bulk of tumors, that possess the ability to self-renew, divide and differentiate into multiple cell lineages. They are able to initiate the formation of a new tumor, leading to tumor recurrence and metastasis following removal of the primary tumor (30).

The interplay between EMT and stemness signature has become increasingly relevant to the field of cancer research. Multiple studies have revealed that cancer stem cell properties may contribute to tumor heterogeneity, maintenance, metastasis, radioresistance and chemoresistance in a various types of cancer (28,31). Such cells have the capacity to give rise to whole tumors due to two fundamental properties: The ability to self-renew, and the ability to differentiate into multiple cell types (32). Critical genes for self-renewal and pluripotency in human embryonic stem cells, including KLF4, SOX2 and OCT4, are likewise elevated in cancer stem cells (33). In addition, the surface glycoprotein CD133 has been identified as a key marker of the cancer stem cell subpopulation in glioblastoma and various types of cancer (23). Consistent with previous reports, SeBT cells exhibited increased expression levels of CD133, SOX2 and OCT4 compared with control and SBT cells. Although it remains unclear why KLF4 expression was decreased in SeBT cells, this reduction may involve the enhanced invasive capability of SeBT cells (34). Cancer stem cells and normal stem cells have been reported to form spheres at increased efficiency compared with differentiated cells (35). The present results obtained from a sphere formation assay demonstrated that SeBT cells were able to form larger spheres compared with control and SBT cells, indicating additional phenotypic changes caused by sequential treatment with low-dose Bix. In conclusion, the results of the present study indicate that SeBT cells induce distant invasion and metastasis through mediation of EMT-promoting markers and that these effects regulate cancer stem cell characteristics in glioblastoma. These findings suggest that SeBT-induced invasion/migration and/or cancer stem cell formation may be major factors contributing to the failure of chemotherapy in glioblastoma patients.

## Acknowledgements

The present study was supported by the Dongnam Institute of Radiological and Medical Science grant funded by the Korean government (grant no. 50590-2015) and the Basic Science Research Program through the National Research Foundation of Korea (grant nos. NRF-2013, M2A2A, 7043665) funded by the Ministry of Science, ICT & Future Planning.

## References

- Lehrer S, Green S, Ramanathan L, Rosenzweig K and Labombardi V: No consistent relationship of glioblastoma incidence and cytomegalovirus seropositivity in whites, blacks, and Hispanics. *Anticancer Res* 32, 1113-1115, 2012.
- Hu Y, Lin X, Wang P, Xue YX, Li Z, Liu LB, Yu B, Feng TD and Liu YH: CRM197 in combination with shRNA interference of VCAM-1 displays enhanced inhibitory effects on human glioblastoma cells. *J Cell Physiol* 220: 1713-1728, 2015.
- Stupp R, Hegi ME, Mason WP, van den Bent MJ, Taphoorn MJ, Janzer RC, Ludwin SK, Allgeier A, Fisher B, Belanger K, *et al*: Effects of radiotherapy with concomitant and adjuvant temozolomide versus radiotherapy alone on survival in glioblastoma in a randomised phase III study: 5-year analysis of the EORTC-NCIC trial. *Lancet Oncol* 10: 459-466, 2009.
- Oberoi RK, Parrish KE, Sio TT, Mittapalli RK, Elmquist WF and Sarkaria JN: Strategies to improve delivery of anticancer drugs across the blood-brain barrier to treat glioblastoma. *Neuro Oncol* 18: 27-36, 2016.
- Jiang WG, Sanders AJ, Katoh M, Ungefroren H, Gieseler F, Prince M, Thompson SK, Zollo M, Spano D, Dhawan P, *et al*: Tissue invasion and metastasis: Molecular, biological and clinical perspectives. *Semin Cancer Biol* 35 (Suppl): S244-S275, 2015.
- Scott RW, Crighton D and Olson MF: Modeling and imaging 3-dimensional collective cell invasion. *J Vis Exp pii*: 3525, 2011.
- Yang J and Weinberg RA: Epithelial-mesenchymal transition: At the crossroads of development and tumor metastasis. *Dev Cell* 14: 818-829, 2008.
- Kalluri R and Weinberg RA: The basics of epithelial-mesenchymal transition. *J Clin Invest* 119: 1420-1428, 2009.
- Li L and Li W: Epithelial-mesenchymal transition in human cancer: Comprehensive reprogramming of metabolism, epigenetics, and differentiation. *Pharmacol Ther* 150: 33-46, 2015.
- Lim J and Thiery JP: Epithelial-mesenchymal transitions: Insights from development. *Development* 139: 3471-3486, 2012.
- Lamouille S, Xu J and Derynck R: Molecular mechanisms of epithelial-mesenchymal transition. *Nat Rev Mol Cell Biol* 15: 178-196, 2014.
- Zang M, Zhang B, Zhang Y, Li J, Su L, Zhu Z, Gu Q, Liu B and Yan M: CEACAM6 promotes gastric cancer invasion and metastasis by inducing epithelial-mesenchymal transition via PI3K/AKT signaling pathway. *PLoS One* 9: e112908, 2014.
- Lo JF, Yu CC, Chiou SH, Huang CY, Jan CI, Lin SC, Liu CJ, Hu WY and Yu YH: The epithelial-mesenchymal transition mediator S100A4 maintains cancer-initiating cells in head and neck cancers. *Cancer Res* 71: 1912-1923, 2011.
- Blick T, Hugo H, Widodo E, Pinto C, Mani SA, Weinberg RA, Neve RM, Lenburg ME and Thompson EW: Epithelial mesenchymal transition traits in human breast cancer cell lines parallel the CD44(hi)/CD24 (lo/-) stem cell phenotype in human breast cancer. *J Mammary Gland Biol Neoplasia* 15: 235-252, 2010.
- Kubicek S, O'Sullivan RJ, August EM, Hickey ER, Zhang Q, Teodoro ML, Rea S, Mechtler K, Kowalski JA, Honan CA, *et al*: Reversal of H3K9me2 by a small-molecule inhibitor for the G9a histone methyltransferase. *Mol Cell* 25: 473-481, 2007.
- Fan JD, Lei PJ, Zheng JY, Wang X, Li S, Liu H, He YL, Wang ZN, Wei G, Zhang X, *et al*: The selective activation of p53 target genes regulated by SMYD2 in BIX-01294 induced autophagy-related cell death. *PLoS One* 10: e0116782, 2015.
- Kim Y, Kim YS, Kim DE, Lee JS, Song JH, Kim HG, Cho DH, Jeong SY, Jin DH, Jang SJ, *et al*: BIX-01294 induces autophagy-associated cell death via EHMT2/G9a dysfunction and intracellular reactive oxygen species production. *Autophagy* 9: 2126-2139, 2013.
- Schmittgen TD, Zakrajsek BA, Mills AG, Gorn V, Singer MJ and Reed MW: Quantitative reverse transcription-polymerase chain reaction to study mRNA decay: Comparison of endpoint and real-time methods. *Anal Biochem* 285: 194-204, 2000.
- Dheda K, Huggett JF, Bustin SA, Johnson MA, Rook G and Zumla A: Validation of housekeeping genes for normalizing RNA expression in real-time PCR. *Biotechniques* 37: 112-114, 2004.
- Uekita T, Tanaka M, Takigahira M, Miyazawa Y, Nakanishi Y, Kanai Y, Yanagihara K and Sakai R: CUB-domain-containing protein 1 regulates peritoneal dissemination of gastric scirrhous carcinoma. *Am J Pathol* 172: 1729-1739, 2008.
- Koukourakis MI, Kalamida D, Giatromanolaki A, Zois CE, Sivridis E, Pouliliou S, Mitrakas A, Gatter KC and Harris AL: Autophagosome proteins LC3A, LC3B and LC3C have distinct subcellular distribution kinetics and expression in cancer cell lines. *PLoS One* 10, e0137675, 2015.
- Wu Y and Zhou BP: New insights of epithelial-mesenchymal transition in cancer metastasis. *Acta Biochim Biophys Sin (Shanghai)* 40: 643-650, 2008.
- Auffinger B, Tobias AL, Han Y, Lee G, Guo D, Dey M, Lesniak MS and Ahmed AU: Conversion of differentiated cancer cells into cancer stem-like cells in a glioblastoma model after primary chemotherapy. *Cell Death Differ* 21: 1119-1131, 2014.

24. Chintala SK, Tonn JC and Rao JS: Matrix metalloproteinases and their biological function in human gliomas. *Int J Dev Neurosci* 17: 495-502, 1999.
25. Schwartzbaum JA, Fisher JL, Aldape KD and Wrensch M: Epidemiology and molecular pathology of glioma. *Nat Clin Pract Neurol* 2: 494-503, 2006; quiz 1 p following 516.
26. Omuro A and DeAngelis LM: Glioblastoma and other malignant gliomas: A clinical review. *Jama* 310: 1842-1850, 2013.
27. Lee JM, Dedhar S, Kalluri R and Thompson EW: The epithelial-mesenchymal transition: New insights in signaling, development, and disease. *J Cell Biol* 172: 973-981, 2006.
28. Singh A and Settleman J: EMT, cancer stem cells and drug resistance: An emerging axis of evil in the war on cancer. *Oncogene* 29: 4741-4751, 2010.
29. Osorio LA, Farfán NM, Castellón EA and Contreras HR: SNAIL transcription factor increases the motility and invasive capacity of prostate cancer cells. *Mol Med Rep* 13: 778-786, 2016.
30. Chow AK, Ng L, Lam CS, Wong SK, Wan TM, Cheng NS, Yau TC, Poon RT and Pang RW: The Enhanced metastatic potential of hepatocellular carcinoma (HCC) cells with sorafenib resistance. *PloS One* 8: e78675, 2013.
31. Colak S and Medema JP: Cancer stem cells-important players in tumor therapy resistance. *FEBS J* 281: 4779-4791, 2014.
32. Reya T, Morrison SJ, Clarke MF and Weissman IL: Stem cells, cancer and cancer stem cells. *Nature* 414: 105-111, 2001.
33. Wang XQ, Ng RK, Ming X, Zhang W, Chen L, Chu AC, Pang R, Lo CM, Tsao SW, Liu X, *et al*: Epigenetic regulation of pluripotent genes mediates stem cell features in human hepatocellular carcinoma and cancer cell lines. *PloS One* 8: e72435, 2013.
34. Zhou Y, Hofstetter WL, He Y, Hu W, Pataer A, Wang L, Wang J, Zhou Y, Yu L, Fang B and Swisher SG: KLF4 inhibition of lung cancer cell invasion by suppression of SPARC expression. *Cancer Biol Ther* 9: 507-513, 2010.
35. Han L, Shi S, Gong T, Zhang Z and Sun X: Cancer stem cells: Therapeutic implications and perspectives in cancer therapy *Acta Pharmaceutica Sinica B* 3: 65-75, 2013.